ORIGINAL

Crab burrow aspect ratio influences particle capture rates on intertidal sandflats

Marine Le Minor [1] · Julia C. Mullarney [2] · Conrad A. Pilditch [2] · Katrin Huhn [1]

Abstract

Crabs are ecosystem engineers that dig burrows, which can trap sediment. We used a field experiment to explore how burrow aspect ratio (depth/diameter) affects the trapping efficiency of sediments and organic material. Arrays of burrows mimics were constructed using tubes of similar depths but two different opening diameters: fat tubes (aspect ratio of 3.8) and thin tubes (7.1). Different arrays were tested to examine whether the combination of burrows with two different aspect ratios affects the material capture, while retaining the same total area of openings per array. The results showed that, in general, the fat tubes trapped more organic material, especially large pieces, and more sediment than thin tubes. Furthermore, the silt-clay content of the sediment trapped in the tubes was up to 50% greater than the surrounding surficial sediment. Hence, we conducted 2D numerical simulations of flow around, and into, a single burrow to elucidate the mechanisms behind particle capture. Results showed that the flushing rate and the turbulent kinetic energy were greater in the fat tubes. However, turbulence persisted for a longer distance downstream of the thin tubes than the fat tubes. The enhanced turbulence may increase the flux of sediment into the tubes where particles can settle and, consequently, promote the sediment capture and sedimentation rate. Our results demonstrate that the aspect ratio of burrows significantly affects capture processes of organic material and sediment particles. Moreover, this capture mechanism depends on the flow regime, as faster flows are associated with larger amounts of material in the water column.

Introduction

Ecosystem engineers are species that modify their environment by altering the flow, changing rates of sediment transport and modifying nutrient cycles. Activities of benthic fauna such as digging, moving and feeding result in sediment mixing and reworking (Graf and Rosenberg 1997; Le Hir et al. 2007), changing surface roughness (Widdows and Brinsley 2002) and modifying the boundary layer above the sediment (Murray et al. 2002). Benthic organisms such as crabs can generate micro-scale topographic features such as mounds, pits, tracks, tubes and burrows, causing changes in benthic seascapes (Meadows et al. 2012).

A common bioturbating species endemic from New Zealand is the tunnelling mud crab *Austrohelice crassa* occupying estuarine soft sediments in the upper intertidal area (Gibbs et al. 2001; Needham et al. 2011). *Austrohelice crassa* is a very active species at both high and low tides and does not remain in its burrow during high tide. Their activities such as burrow building for protection against predators modify the sediment-water interface as well as the water flow and fluid infiltration. Exchanges between the water and sediment are enhanced owing to the larger sediment-water boundary surface area within the burrows (Ziebis et al. 1996; Laverock et al. 2011; Needham et al. 2011). Burrows alter nutrient cycles: key nutrients such as oxygen and nitrogen are transported by the water entering and moving through these holes and flowing through the sediment. It is well established that burrows contribute significantly to the release of ammonium into the environment (Vopel and Hancock 2005). Furthermore, a larger density of burrows enhances oxygen uptake by sediment (Ziebis et al. 1996; Gilbert et al. 2003). Additionally, crab burrows play a key role in the stabilization of sediment beds (Needham et al. 2013). Consequently, mud crabs are ecosystem engineers and considered as key species in their

✉ Marine Le Minor
mleminor@marum.de

[1] MARUM - Center for Marine Environmental Sciences, University of Bremen, Leobener Str. 8, 26359 Bremen, Germany

[2] Coastal Marine Group, School of Science, University of Waikato, Private Bag 3105, Hamilton 3240, New Zealand

natural environments (Warren and Underwood 1986; Thrush et al. 2003; Needham et al. 2011).

Heron and Ridd (2001) investigated the influence of flow induced by tides on the flushing rates of animal burrows with varying complexities (depth, geometry, number of apertures). Burrows with multiple apertures have not been proven to be more easily flushed than burrows with several loops (Heron and Ridd 2003, 2008). The flushing rate is also related to the features on the bed (micro-topography) that may redirect the flow into the burrows (i.e. irrigation; Ziebis et al. 1996); these features result from organism activity such as burrowing and maintenance activities of mud crabs.

The size, shape and density of the tunnelling mud crab burrows depend on the environmental conditions and sediment type (Kristensen and Kostka 2005). Burrows of *Austrohelice crassa* can have many different shapes: cone, u-, j-, i-, y-, inverted y-, branching or complex shapes forming galleries of tunnels (Morrisey et al. 1999; Needham et al. 2010). In fact, the burrows dug by the mud crabs may also be interconnected, which means that one burrow can have more than one entrance and form a network similar to arteries (Vopel and Hancock 2005). Moreover, *Austrohelice crassa* adapts its building behaviour to the sediment properties (Needham et al. 2013): in muddy sediment, the burrows often have a i- or j- shape with a median depth of 47 mm whereas, in sandy sediment, the burrows often present a j-, i- or inverted y- shape with a median depth of 39 mm (Needham et al. 2010). The diameter of mud crab adult burrows is generally greater than 8 mm (Needham et al. 2013). The burrow volume, surface area and complexity are, thus, greater in muddy than in sandy sediment (Morrisey et al. 1999). Simple burrows are often characterised by the aspect ratio, defined as the ratio between the cavity depth and the cavity diameter (at its opening). The median aspect ratio is, consequently, 6 in muddy sediment and 5 in sandy sediment.

In the 1980s, numerous studies were conducted regarding the efficiency of sediment traps and aimed at qualifying and quantifying the impact of the shape and aspect ratio on the sediment capture mechanism (Gardner 1980a, 1980b, 1985; Butman 1986; Butman et al. 1986). In particular, cylindrical sediment traps have been studied by researchers to evaluate their efficiency to collect the sinking particles in the water column. It has been shown that crab holes catch sediment, retain detritus and trap organic matter (Iribarne et al. 2000). Particles of organic matter and sediment grains can be transported into burrows with the flow. By altering the hydro- and sediment dynamics, crabs can enhance material trapping in the burrows they dig. When the sediment capture is a selective process, meaning that fine sediment particles (silt-clay) are trapped in burrows and, then, incorporated into sands, the sediment grain size distribution may be altered causing fundamental changes in sediment erosion (van Katwijk et al. 2010). Pore water exchange may, as a consequence, change enhancing the modification of nutrient cycles and faunal composition.

Investigations reveal that the burrow morphology influences sediment trapping with funnel-shaped burrow apertures capturing twice as many particles than tubular openings (Escapa et al. 2008). In this case, the number of particles transported as bedload and caught within funnel-shaped burrow entrances is also larger (Witbaard and Duineveld 1989; Nickell et al. 1995; Iribarne et al. 1997; Botto et al. 2006). It has also been established that pits enhance sediment deposition and, therefore, increase the food supply to their inhabitants (Yager et al. 1993). Similar results have been observed for sediment traps.

Only a few studies have been focused on the influence of the density of cavities such as crab burrows on the water flow and the associated sediment transport (Needham et al. 2013). Most of the studies on burrow trapping efficiency have focused on single features only. Nevertheless, the density of mud crab *Austrohelice crassa* burrows ranges from 30 burrows·m^{-2} in sand to 207 burrows·m^{-2} in mud (Needham et al. 2010). For a burrow density increasing from 100 to 400 burrows·m^{-2} in mud and from 19 to 100 burrows·m^{-2} in sand, a clear transition from erosion to deposition has been observed under flow speeds varying from 5 to 45 cm·s^{-1} (Needham et al. 2013). The role of interactions between burrows, particularly burrow aspect ratios, and their combined effects are not well known. However, one of the very few studies of multiple biogenic structures such as pits did report a transition from erosion to deposition for an increasing percentage of sediment bed covered (Friedrichs et al. 2009).

The present study therefore aims to (i) determine whether crab burrow aspect ratio influences sediment deposition, (ii) determine if there is a combination (array) of crab burrows with different aspect ratios that is more efficient at catching organics and collecting sediment, and (iii), to establish whether the sediment trapping by crab burrows is a selective process. These objectives are addressed through field experiments in Tairua, New Zealand, where tunnelling mud crabs *Austrohelice crassa* are found in abundance. The field measurements allow us to quantify the amounts of organics and sediment captured over one tidal cycle in mimicked crab burrows. These collected data serve, therefore, to assess the trapping efficiency of crab burrow according to their aspect ratio under different flow regime such as hydrodynamic and wave conditions. To gain an insight into the mechanisms behind the flow capture by simulating the flow around and into a single burrow afterwards, numerical simulations are used.

Methods

The fieldwork was carried out on 29th and 30th July 2017, in a sheltered sub-estuary in Tairua, New Zealand (GPS

coordinates: 175° 50' 49" E and 37° 0' 9" S). This estuary with tidal ranges ≤ 2 m is characterised by intertidal sand- and mudflats, which are populated by a large number of *Austrohelice crassa* mud crabs (Needham et al. 2010, 2011, 2013).

Burrow arrays

Centrifuge tubes with a conical bottom were used to mimic natural crab burrows. These polypropylene tubes exhibited the i-shape that is one of the most common shape of natural mud crab burrows in sandy sediment (Needham et al. 2010, 2011, 2013). Two different sized tubes were used: 15 mL and 50 mL tubes. Both sizes had similar lengths of approx. 120 mm, but different opening diameters 17 and 30 mm, to yield burrow aspect ratios of 7.1 and 3.8 for 15 mL and 50 mL tubes, respectively. Hereafter, we refer to the 15 mL and 50 mL tubes as thin and fat tubes, respectively.

The tubes were distributed into four different configurations within a 1-m^2 array, each 1 m apart from each other (Fig. 1a). In order to see how the aspect ratio affects the sediment trapping process, the total surface occupied by the tube openings was kept constant for the four different arrays, i.e. around 0.016 m^2; however, the combination of fat and thin tubes differed (Fig. 1b). Two cases of mixed arrays were tested: Mixed-F with 16 fat tubes which cover 70% of the opening area and 21 thin tubes covering 30% respectively; and a Mixed-T array with only 7 fat tubes and 49 thin tubes and the inverse ration of 30% fat tubes and 70% thin tubes covering the opening surface. In addition, two unmixed cases were analysed where arrays contained only fat or only thin tubes (Unmixed-F with 100% or 23 fat tubes and Unmixed-T with 100% or 70 thin tubes; Fig. 1b). Hence, in total, 372 tubes mimicking burrows were deployed: 46 fat tubes and 140 thin distributed between the four array scenarios for each day of fieldwork. A bare plot with neither fat nor thin tubes was used as a control array both days (Fig. 1a).

The arrays were deployed for one tidal cycle and repeated the following day to examine the effects of different hydrodynamic conditions. Prior to tidal inundation, the tubes were filled with filtered seawater and closed with a screw cap. Tubes were manually pushed in the sand with x and y positions within each array determined using a random number generator. Just before the rising tide flushed the tubes, the screw caps were removed and the tubes set in the sandy sediment with their openings level with the surrounding substrate.

Sediment data collection and processing

Two rectangular tiles of dimensions 76 × 152 mm were placed level with the sediment surface in each array (Fig. 1b, c). Tiles were deposited with the rough side up facing the flow to enable particle collection and thus to estimate the

sedimentation rate or background deposition rate respectively of each array during a tidal cycle. After the experiment, tiles were recovered for further analysis in the laboratory. Each tile was washed with fresh water above pre-weighed and dried filter papers within a vacuum apparatus. The filter papers with the sediment were placed in an oven for 24 h at 105 °C and then weighed. The weight provided an estimate of the amount of sediment deposited in each array. Unfortunately, the amount of sediment that was deposited on the tiles was not large enough to run a grain size analysis.

To gain an overview about the general sedimentological conditions in the target area in the vicinity of the array, grab samples of surface sediment were taken to obtain grain sizes of the marine surficial sediment from our field site. Half of these samples were digested in 10% hydrogen peroxide to remove organic matter while the second half were kept intact before being placed in the Malvern Mastersizer 2000 to obtain grain size.

Hydrodynamic instruments and processing

A set of instruments was deployed in the vicinity of the arrays each day of the field experiment (Fig. 1a, b). Instruments were deployed at the bed around 8 m in front of the tube arrays. Under the slow conditions observed during the experiments, the impact of the frames on the sediment dynamics was considered to be negligible. The instruments consisted of:

(I) An RBR Concerto CTD (conductivity temperature depth profiler; Fig. 1a) was used to record pressure data at a frequency of 6 Hz. The instrument was placed in front of the row of arrays at 9.5 cm and 9 cm above the bed on day 1 and day 2, respectively, and. Water depths were given at 1-min intervals following removal of atmospheric pressure fluctuations and averaging.

(II) A 2-MHz Nortek Aquadopp ADCP (Acoustic Doppler Current Profilers) operating in downward-looking pulse-coherent mode was employed to measure the flow velocities and pressure (Fig. 1a). This Aquadopp sampled at a 2.5-cm vertical resolution over a profile of 33 cm and 26 cm above the bed on day 1 and day 2, respectively. Data were collected at 8 Hz to show the flow field. Measurements were taken above the Mixed-F array on day 1 and Unmixed-T on day 2. The data collection lasted from the moment the ADCP was submerged by flooding tide until they emerged at the end of ebb tide, e.g. 11:00 to 13:00 on day 1.

(III) Three Vectrino profilers were utilised (Fig. 1c). The probes were placed above the control array and the two unmixed arrays on day 1 and above the control array and the two mixed arrays on day 2 (Fig. 1a, b). Vectrino profilers recorded data continuously at 50 Hz over a ~25-mm-long vertical profile near the sediment
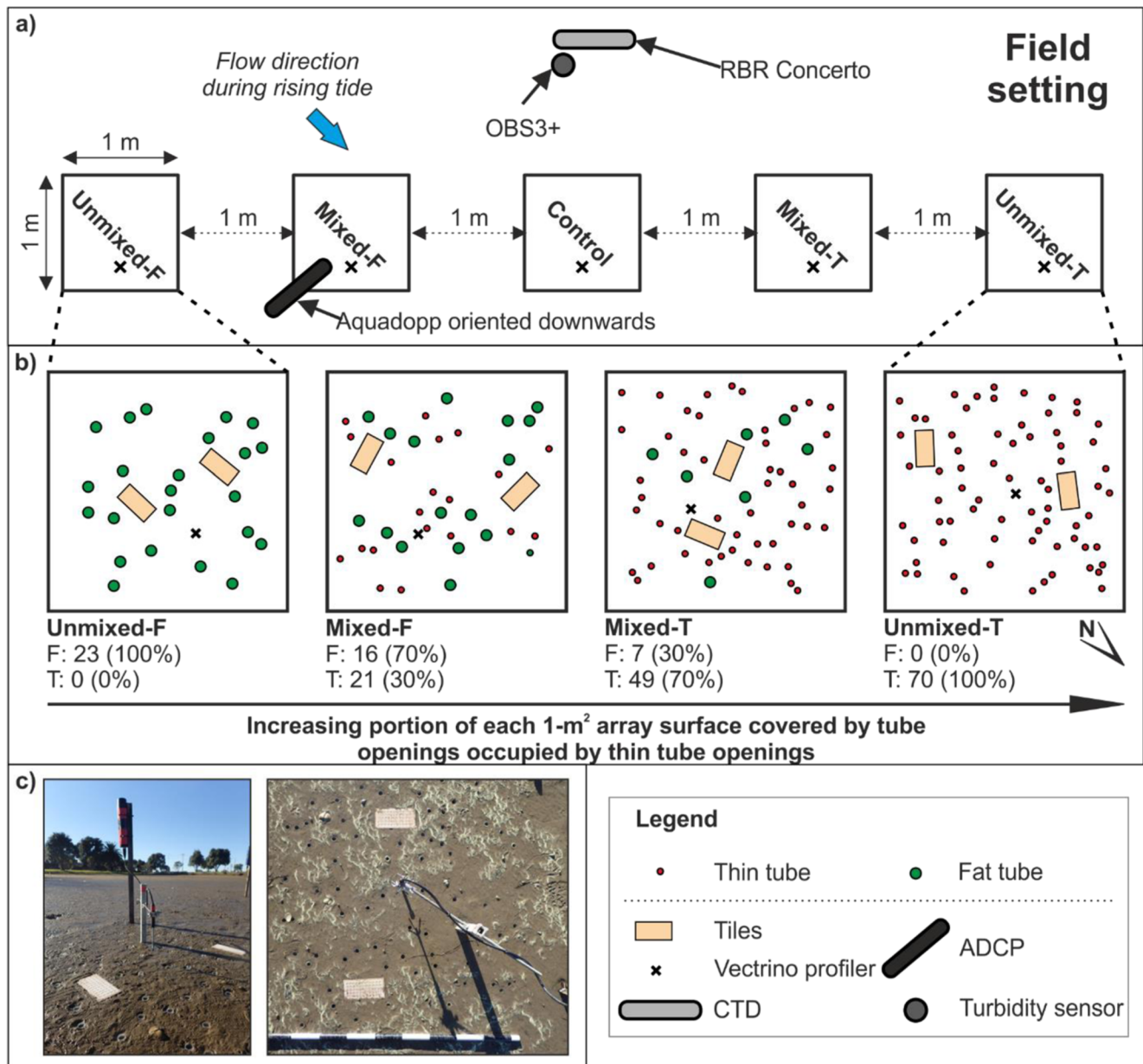
Fig. 1 Experimental setup. **a** Set of arrays deployed in the field. In total, five arrays were deployed on each day of field experiment. Four arrays contained tubes while the fifth array was free of tubes to serve as a control array. Although the number of fat and thin tubes changed between the four arrays, the total area covered by the tubes was kept constant (around 0.016 m²). The arrays with tubes were labelled as follows: Unmixed-F (100% of the opening area covered by fat tubes), Mixed-F (70% of the opening area covered by fat tubes and the remaining opening surface by thin tubes), Mixed-T (70% of the opening area covered by thin tubes and the remaining opening surface by fat tubes) and Unmixed-T (100% of the opening area covered by thin tubes). **b** Top view of the distribution of burrow mimics within each array. **c** Side view and top view of a Vectrino profiler above Unmixed-T. The scale bar was removed before inundation

bed (resolution of 1 mm). The data collection lasted from the moment the Vectrino profilers were submerged by flooding tide until they emerged at the end of ebb tide, e.g. from 10:00 to 14:00 on day 1.

For both ADCP and Vectrino profilers, data with beam correlations of less than 70% were removed. Turbulent kinetic energy (TKE) dissipation rates (ε in W·kg^{-1}) were calculated using Vectrino data over 10-min intervals along vertical beams

using the structure function method of Wiles et al. (2006). The ADCP and Vectrino velocity data were averaged over 1-min intervals.

(IV) An optical backscatter sensor (Campbell Scientific OBS3+) was placed outside the arrays to measure the turbidity (Fig. 1a) at heights 5.5 cm and 4.5 cm above bed on day 1 and day 2, respectively. Turbidities were converted to total suspended solids (TSS) through a

laboratory calibration using samples of surficial sediments taken from the field site (after sieving it through a 250-µm mesh to remove the coarse grains that are unlikely to be re-suspended).

Material trapped in burrows—data analyses and processing

After a tidal cycle, tubes were closed with a lid and retrieved. In the laboratory, the content of each tube was filtered using a 1-mm mesh to remove macro-organics (e.g. algae, seagrasses) and macrofauna such as tunnelling mud crabs from the sediment. All animals found in the tubes were counted and identified. A crab was considered as adult when its carapace width was larger than 5 mm and juvenile otherwise (Needham et al. 2010). Organic material was placed in the oven for 2 days at 60 °C, and subsequently weighed to obtain the dry weight of the organics caught in each tube referred to as macro-organic catching (in mg) hereafter. The deposition rates of macro-organics (in mg·cm^{-2}) were estimated for each tube by dividing the mass of macro-organic trapped by the tube opening area.

The remaining seawater and sediments in the tubes were spun for 10 min at a speed of 3300 rotations per minute in a centrifuge to separate sediments from seawater. Afterwards, seawater was discarded and tubes were filled with freshwater and centrifuged again to remove salt. After discarding the salted water, tubes were placed in the oven for 2 days at 60 °C. Dry weight of the sediment trapped in each tube, referred to as sediment trapping (in mg), was then measured. Subsequently, sediment deposition rates (in mg·cm^{-2}) were estimated for each tube by dividing the mass of sediment trapped by the tube opening area.

After these measurements of sediment deposition rate per tube, sediment content of half of the tubes from an array was used to conduct grain size analyses, whereas the other half was used to determine the organic matter content (e.g. in case of Unmixed-T 35 thin tubes for grain size analyses and 35 for organic matter). In case of mixed arrays (Mixed-T and Mixed-F), half of the fat tubes were analysed for grain sizes and the other half of fat tubes for organic matter; and in the same way, half of the thin tubes for one or the other. Therefore, both aspect ratios were always handled and analysed independently. The grain size analyses reveal a median diameter d_{50} and percentage of silt-clay, i.e. < 63 µm of the undigested sediment trapped in the tubes (Malvern Mastersizer 2000), while the remaining matter was used in loss-on-ignition to obtain an estimate of the total organic matter (contents of several tubes were placed in the furnace for 8 h at 550 °C and eventually weighed). The sediment analyses were repeated to estimate the variability of the sediment properties.

To assess the significance of these measurements, statistical analyses were conducted. Macro-organics catching, macro-organics deposition rates, sediment trapping, sediment deposition rates and sediment properties (median diameter, silt-clay and organic matter contents) were used as indicators of capture efficiency for statistical analyses across the two aspect ratios using Matlab. Before any statistical analysis, outliers were removed according to the 1.5xIQR rule, i.e. data below the first quartile and above the third quartile were not considered for further statistical tests. Within each array, differences of macro-organics catching, sediment trapping values, fines content and organic matter content among aspect ratio were analysed using t-test for unpaired samples with unequal variance. We considered the null hypothesis that the indicators mentioned above had equal means for both tube aspect ratios. The results from t-tests, i.e. probability values noted p, provided weak or strong evidence against this null hypothesis: small p values indicated that the data were not consistent with the null hypothesis ($p < 0.05$, 95% confidence level), and thus, this hypothesis was rejected.

Two-way ANOVA (ANalysis Of VAriance) was conducted to assess if there were differences between the aspect ratios in macro-organics catching/deposition rates, sediment trapping/deposition rates, fines content and organic matter content values as a function of treatment (array) were statistically significant at 95% confidence level ($p = 0.05$). This statistical test was unbalanced since the number of fat and thin tubes differed between treatments i.e. arrays.

A chi-square test was also run to determine if the arrays significantly affected the distribution of macro-organics and sediment between fat and thin tubes at the 95% confidence level ($p = 0.05$).

Numerical simulations

Limitations in technology prevent direct observation of the capture mechanism of burrows during field experiments. Therefore, we utilised a 2D numerical model to examine the processes leading to potential differences in material trapping efficiency between tubes with different aspect ratio and to aid in the interpretation of the field measurements. Flow conditions in and around crab burrows of different aspect ratios were simulated using the computational fluid dynamics toolbox OpenFOAM (Open Field Operation and Manipulation). OpenFOAM is an open source code based on a finite volume approach using a solver for incompressible fluids (for further details, please see Le Minor et al. (2019)). The numerical model presented here was validated against published data (cf. procedure and results in Appendix A).

The 2D rectangular numerical model (50 cm in length and 30 cm height above bed) mimics a vertical cross section through the water column and the shallow sediment bed. A buried tube or crab burrow respectively was simplified as a

rectangular box inserted at the bottom of the computational domain. "Tube" dimensions are identical to the tubes used in the field experiments: 120 mm in height and 17 mm and 30 mm in width in case of thin and fat tubes, respectively. The computational domain consisted of a uniform hexahedral mesh with a uniform mesh resolution of 0.5 mm. This box was fully flooded during all experiment runs. Tidal flow conditions were simulated by applying a constant inflow at the left vertical side of the domain (inlet) and exited the box on the right (outlet). A typical logarithmic velocity profile was mapped at the inlet with a downstream velocity of 10 cm·s^{-1} which was in the same range as field observations (e.g. Fig. 2). The flow profile was generated using the Spalding's law of the wall (Spalding 1961). To simulate burrow generated turbulence in the water column, the Large-Eddy simulation (LES) approach with the one equation eddy-viscosity model was used. This approach has been previously utilised to successfully resolve large-scale eddies and simulate small-scale eddies (Palau-Salvador et al. 2010). Experiments were run for a duration of 300 s and a time step of 1 ms to ensure the stability of the calculations.

Results

Hydrodynamics and total suspended solids

The hydrodynamic conditions above the different arrays are shown during a tidal cycle for both days (Fig. 2). The water depth changed over the tidal cycle, reaching 62 cm on day 1 and 50 cm on day 2 at high tide (Fig. 2a, e). Overall, horizontal flow velocities were faster during the ebb tide on both days of the field experiment. Velocities measured by the downward-looking Aquadopp reached values of 17 cm·s^{-1} on day 1, while the maximum flow speed was 11 cm·s^{-1} on day 2 (Fig. 2a, e). Near-bed horizontal flow speeds (from the Vectrino profilers) reached up to 12 cm·s^{-1} on both days (Fig. 2b–d, f–h). Fastest flow speeds were observed during ebb tide on both days; however, high values were also measured during flood tide on day 2. In general, the turbulent dissipation rate was around $O(10^{-7}–10^{-5}$ W·kg^{-1}) (not shown).

In brief, the hydrodynamic conditions, i.e. flow velocities and dissipation rate of turbulent kinetic energy (not shown), did not vary significantly between arrays, and between arrays fluctuations were much smaller than the changes over time. Furthermore, the flow conditions were slightly more energetic on day 1, with wind-waves reaching a height of a couple of centimetres (personal observations) while the water surface was relatively smooth on day 2.

Near-bed total suspended solids (TSS) was measured directly in front of the arrays during both days (Fig. 2). Values were very low, around 5 mg·L^{-1}, for the majority of both tidal cycles. Almost no fluctuations could be observed before and after slack tide rather the TSS stayed uniform over the entire tidal cycle (Fig. 2). However, the TSS exhibited a sharp increase at the ebb tide on day 1 from 13:00 (Fig. 2a).

Material capture in the tubes

Macrofauna

Many tubes contained macrofauna and all the individuals caught were counted and identified (Table 1). The tunnelling mud crab *Austrohelice crassa* and estuarine pillbox crab *Halicarcinus whitei* were the most frequent species retrieved from the tubes. Overall, a larger number of crabs were caught on day 1 with 28 (17 juveniles and 11 adults) than on day 2 (24 crabs, of which 9 were juveniles and 15 were adults).

To compare the impact of tube aspect ratio on the presence of macrofauna, three ratios were computed for each array: the number of (a) individuals, (b) adult and (c) juvenile crabs found in tubes with the same aspect ratio were divided by the number of tubes with this same aspect ratio to give the average number caught per tube (Table 1). E.g. on day 1, in the unmixed arrays, in total, 0.13 macrofauna or in particular 0.00 adult crabs and 0.07 juvenile crabs were found in thin tubes. Hence, the ratio smaller than 1 means that there were fewer crabs collected than the number tubes (i.e. some tubes did not capture any macrofaunal organisms).

Overall, fat tubes had a greater catch rate than thin tubes, with the exception that more individuals particularly both adult and juvenile crabs were found in thin tubes in the unmixed and Mixed-T arrays on day 2 (Table 1).

Trapping of macro-organics

In addition to crabs, the tubes mimicking crab burrows captured other organic matter. The larger material (> 1 mm), obtained after sieving the tube content and removing the macrofauna, mainly consisted of seaweeds and plants. In general, the dry weight of large organic material captured in the tubes was significantly higher on day 1 than on day 2 ($p = 0.0000$ from t-test; see also y-axes in Fig. 3).

Within each array, the difference in capture of macro-organics between the two tube aspect ratios was significant according to t-test results for both days (Table 2). In Mixed-F, fat tubes trapped larger amounts of macro-organics than thin tubes: 106.0 mg against 23.9 mg ($p = 0.0000$) on day 1 and 5.7 mg agains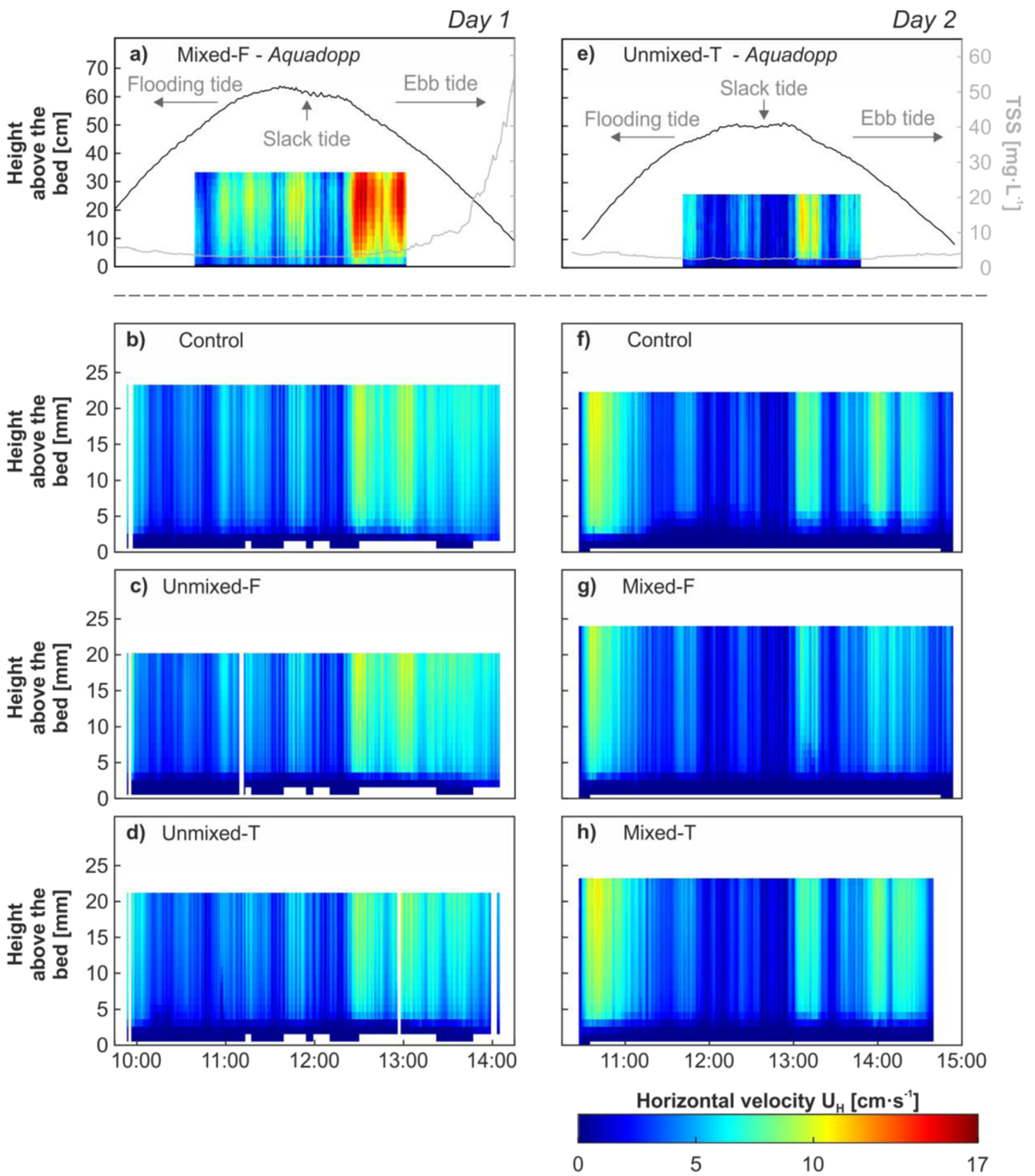t 0.5 mg on day 2 ($p = 0.0000$, Fig. 3a, e). The same contrast between fat and thin tubes applies to the unmixed arrays, where fat tubes also trapped larger amounts of macro-organics than thin tubes: 62.4 mg against 18.3 mg ($p = 0.0000$) on day 1 and 4.6 mg against 0.9 mg ($p = 0.0000$, Fig. 3a, e).

Fig. 2 Horizontal velocities in cm·s^{-1} observed on day 1 (a–d) and day 2 (e–h) of fieldwork. Graphs (a) and (e) correspond to the horizontal velocities measured with downward-looking Aquadopp above Mixed-F on day 1 and Unmixed-T on day 2, respectively. Black lines indicate water level measured with the CTD and grey lines correspond to the total suspended solids (TSS) in mg·L^{-1} measured with a turbidity sensor placed 5.5 cm above the bed on day 1 and 4.5 cm above the bed on day 2. Horizontal velocities acquired with Vectrino profilers above the control array are shown in (b) and (f) whereas (c) and (d) show above Unmixed-F and Unmixed-T measured on day 1, and (g) and (h) above Mixed-F and Mixed-T on day 2, respectively

Table 1 Macrofauna (average number of individuals per tube type within each array) caught split into tubes with two different aspect ratios and split into general individuals, adult and juvenile crabs

Day	Array	(a) Number of individuals		(b) Adult crabs		(c) Juvenile crabs	
		Fat	Thin	Fat	Thin	Fat	Thin
Day 1	Unmixed	7 (0.30)	9 (0.13)	2 (0.09)	0 (0.00)	1 (0.04)	5 (0.07)
	Mixed-F	8 (0.50)	3 (0.14)	2 (0.13)	2 (0.10)	4 (0.25)	1 (0.05)
	Mixed-T	3 (0.43)	11 (0.22)	1 (0.14)	4 (0.08)	2 (0.29)	4 (0.08)
Day 2	Unmixed	2 (0.09)	13 (0.19)	2 (0.09)	9 (0.13)	0 (0.00)	4 (0.06)
	Mixed-F	6 (0.38)	1 (0.05)	2 (0.13)	0 (0.00)	3 (0.19)	1 (0.05)
	Mixed-T	0 (0.00)	7 (0.14)	0 (0.00)	2 (0.04)	0 (0.00)	1 (0.02)

After comparing fat tubes and thin tubes within each array for both days, a two-way ANOVA was run on 177 and 154 tubes out of 186 on day 1 and day 2, respectively, to shed light on the effect of aspect ratio and array on macro-organics catching (Table 3). There was a significant interaction between the effects of aspect ratio and array on trapping of macro-organics. This significance is shown in Table 3 by the p and F-values: $F(2,172) = 3.41$, $p = 0.0354$ on day 1 and $F(2,149) = 5.11$, $p = 0.0071$ on day 2. On day 1, simple main effects analysis showed (Table 2) that fat tubes had significantly larger deposition rates of macro-organics than thin tubes when located in Mixed-F array ($p = 0.0041$), but there were no differences between aspect ratio when placed in unmixed arrays (because $p = 0.4689$) or Mixed-T ($p = 0.1311$) both $p > 0.05$.

On day 2, simple main effects analysis showed that fat tubes again had significantly larger deposition rates of macro-organics than thin tubes when located in Mixed-F array ($p = 0.0004$). In contrast, a significant correlation of aspect ratio and catching could also identified for the unmixed arrays ($p = 0.0179$) on day 2. However similar to day 1, in Mixed-T ($p = 0.9390$), there were no differences between aspect ratio and catching. In summary, fat tubes exhibited larger deposition rates of macro-organics than thin tubes in unmixed arrays, e.g. 0.6 mg·cm^{-2} against 0.4 mg·cm^{-2} on day 2 (Fig. 3f).

Arrays with fat tubes caught greater amounts of macro-organics (Fig. 4a, c). The highest amount of macro-organics was trapped in Mixed-F array followed by Unmixed-F on both days. In Mixed-F, 0.238 mg·cm^{-2} of organic material was deposited on day 1, and 0.014 mg·cm^{-2} on day 2. In Unmixed-F, the deposition rate of macro-organics in fat tubes was 0.173 mg·cm^{-2} on day 1 and 0.012 mg·cm^{-2} on day 2. Unmixed-T and Mixed-T therefore appeared to be less efficient at capturing organics. Indeed, in Unmixed-T, the deposition rate of macro-organics in thin tubes was 0.146 mg·cm^{-2} on day 1 and 0.007 mg·cm^{-2} on day 2. In Mixed-T, 0.089 mg·cm^{-2} of organic material was deposited on day 1 and 0.009 mg·cm^{-2} on day 2. These observations are regarded as statistically different because the amounts of macro-organics

caught in the tubes were significantly contrasting between the 2 days ($p = 0.0000$). Mixed arrays significantly affected the distribution of macro-organics between fat and thin tubes on both days ($p = 0.0001$ on day 1 and $p = 0.0000$ in day 2, Fig. 4a, c). In Mixed-F, the distribution was as follows: 28.72% in thin tubes and 71.28% in fat tubes on day 1 but 6.92% in thin tubes and 93.08% in fat tubes on day 2. In Mixed-T, the distribution was as follows: 55.77% in thin tubes and 44.23% in fat tubes on day 1 and, similarly, 53.53% in thin tubes and 46.47% in fat tubes on day 2. Therefore, in Mixed-T, fat tubes captured relatively more macro-organics for their surface area than the thin tubes.

Sediment trapping in tubes and sediment properties

In addition to the macrofauna and the large organic material, the tubes also trapped sediment. In general, the dry weight of sediment caught in the tubes was larger on day 1 than on day 2 with the amount trapped on average 3 times larger on day 1 than on day 2 for both the thin and the fat tubes ($p = 0.0000$ from t-test, Fig. 3c, g). Within each array, the difference in sediment capture between the two tube aspect ratios was significant on both days (Table 2). In unmixed arrays, fat tubes trapped higher amounts of sediment than thin tubes: 280.2 mg against 156.6 mg ($p = 0.0005$) on day 1 and 55.0 mg against 41.0 mg on day 2 ($p = 0.0237$, Fig. 3c, g).

A two-way ANOVA was also run on a sample of 175 and 167 tubes to examine the effect of aspect ratio and array on sediment trapping, on day 1 and day 2, respectively (Table 3). There was a significant interaction between the effects of aspect ratio and array on sediment trapping, $F(2,170) = 5.61$, $p = 0.0044$ on day 1 and $F(2,162) = 5.59$, $p = 0.0045$ on day 2. On day 1, simple main effects analysis showed that thin tubes had significantly larger sediment deposition rates than fat tubes when located in Mixed-T array ($p = 0.0472$) and in unmixed arrays ($p = 0.0000$), but there were no differences between aspect ratio when placed in Mixed-F ($p = 0.0816$). On day 2, simple main effects analysis showed that thin tubes had significantly higher sediment deposition rates than fat
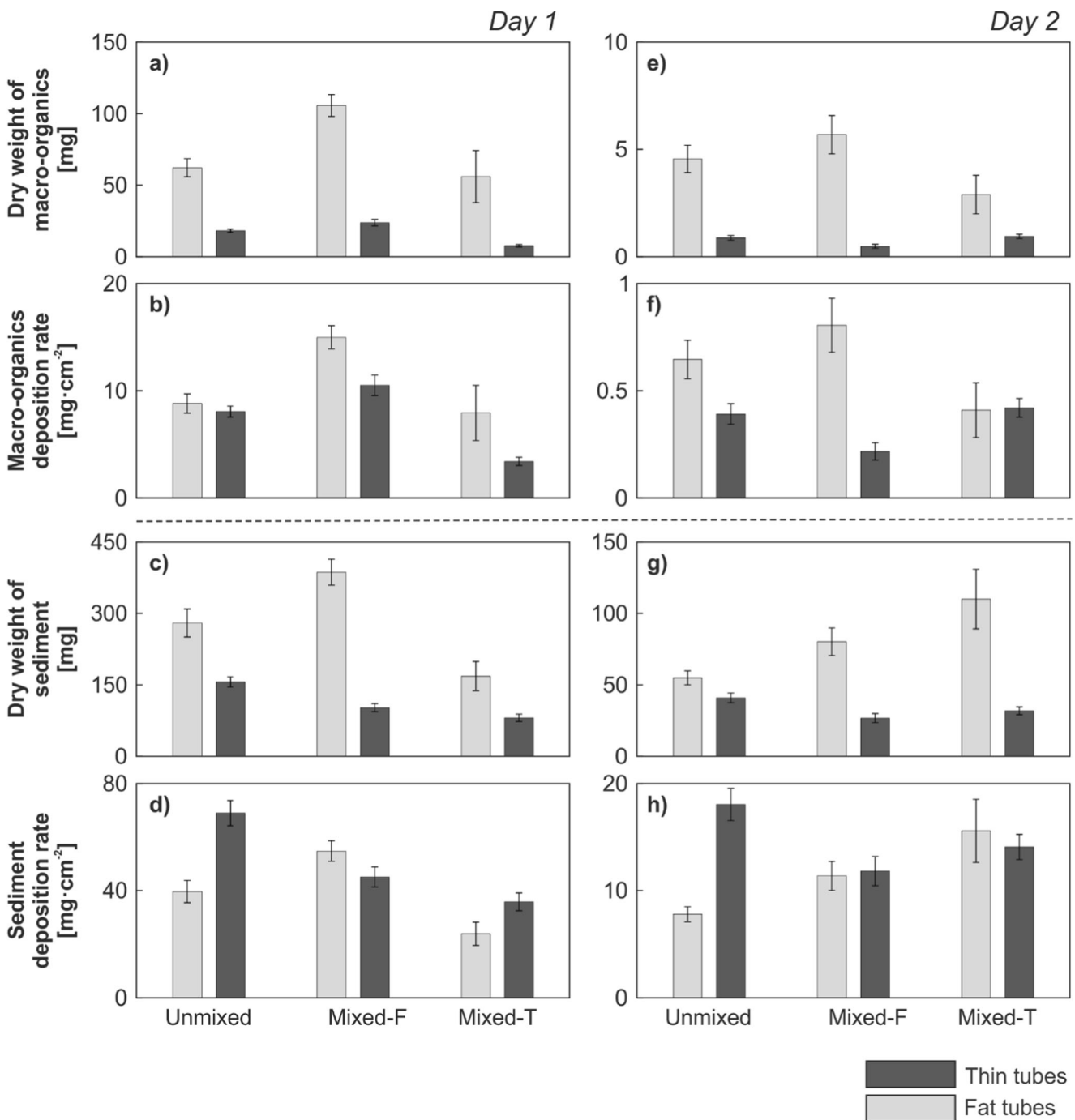
Fig. 3 Amounts and deposition rates of macro-organic material and sediment captured in tubes on day 1 (**a–d**) and day 2 (**e–h**). The light grey bars correspond to fat tubes and the dark grey bars correspond to thin tubes. Graphs (**a**) and (**e**) show the average amounts (dry weight) of macro-organics caught per tube. Graphs (**b**) and (**f**) show the average deposition rates of macro-organics per unit area. Graphs (**c**) and (**g**) show the average amounts (dry weight) of sediment trapped per tube. Graphs (**d**) and (**h**) show the average deposition rates of sediment per unit area of tube opening. The different arrays are sorted along the horizontal axis. Vertical lines plotted at the top of the bars correspond to the standard errors associated to each sample after removing outliers according to the 1.5xIQR rule

tubes when located in unmixed arrays ($p = 0.0000$), but there were no differences between aspect ratio when placed in Mixed-F ($p = 0.8138$) or and in Mixed-T ($p = 0.6483$). Indeed, in unmixed arrays, fat tubes exhibited smaller deposition rates of sediment than thin tubes: 39.6 mg·cm^{-2} compared to 69.0 mg·cm^{-2} on day 1 and 7.8 mg·cm^{-2} compared to 18.1 mg·cm^{-2} on day 2 (Fig. 3d, h).

In general, greater sediment trapping was positively correlated to a larger number of thin tubes, and therefore, fewer fat tubes. On both days, the largest amount of sediment was

Table 2 Results of *t*-test assuming unequal variance to assess the impact of aspect ratio on capture and deposition rates of macro-organics and sediment as well as trapped sediment properties. We considered the null hypothesis that, for both tube aspect ratios, the macro-organics catching, macro-organics deposition rates, sediment trapping, sediment deposition rates and sediment properties (median diameter, silt-clay and organic matter contents) had equal means. Small *p* values in italics indicate that the data are not consistent with the null hypothesis ($p < 0.05$, 95% confidence level) and, thus, this hypothesis may be rejected

Day 1	Macro-organics catching	Macro-organics deposition rates	Sediment trapping	Sediment deposition rates	Silt-clay content	Organic matter content	d_{50}
Unmixed	*0.0000*	0.4689	*0.0005*	*0.0000*	*0.0016*	*0.0022*	*0.0007*
Mixed-F	*0.0000*	*0.0041*	*0.0000*	0.0816	0.2231	*0.0293*	*0.0475*
Mixed-T	*0.0377*	0.1311	*0.0290*	*0.0472*	–	0.2711	–

Day 2	Macro-organics catching	Macro-organics deposition rates	Sediment trapping	Sediment deposition rates	Silt-clay content	Organic matter content	d_{50}
Unmixed	*0.0000*	*0.0179*	*0.0237*	*0.0000*	0.8273	*0.0000*	0.3148
Mixed-F	*0.0001*	*0.0004*	*0.0001*	0.8138	0.1692	0.6226	0.4336
Mixed-T	0.0842	0.9390	*0.0094*	0.6483	0.3395	0.4456	0.6094

deposited in Unmixed-T (Fig. 4b, d). Indeed, in unmixed arrays, the deposition rate of sediment in Unmixed-T was 1.39 mg·cm^{-2} on day 1 and 0.58 mg·cm^{-2} on day 2 when, in Unmixed-F, it was 0.64 mg·cm^{-2} on day 1 and 0.14 mg·cm^{-2} on day 2. In Mixed-F, 0.90 mg·cm^{-2} of sediment was deposited on day 1 and 0.25 mg·cm^{-2} on day 2. As for Mixed-T, 0.58 mg·cm^{-2} of sediment was deposited on day 1 and 0.32 mg·cm^{-2} on day 2. These observations are regarded as statistically different since the amounts of sediment trapped in the tubes were significantly contrasting between the 2 days ($p = 0.0000$).

In mixed arrays, the amount of trapped sediment was distributed between the fat and thin tubes. These arrays significantly affected the distribution of sediment between fat and thin tubes on both days ($p = 0.0000$ on both days). In Mixed-F, where 30% of the surface occupied by the tube openings correspond to thin tubes and 70% to fat tubes, the distribution was as follows: 26.05% in thin tubes and 73.95% in fat tubes on day 1 and 25.97% in thin tubes and 74.03% in fat tubes on day 2. In Mixed-T, where 70% of the surface occupied by the tube openings correspond to thin tubes and 30% to fat tubes, the distribution was as follows: 79.51% in thin tubes and 20.49% in fat tubes on day 1 and 75.55% in thin tubes and 24.45% in fat tubes on day 2.

The properties of the sediment captured in the tubes were analysed to explore any dependence on aspect ratio (Table 4). Firstly, the organic matter content was slightly larger on day 1 than on day 2: 7.19% against 5.61% when results from all the tubes are considered. On day 1, the thin tubes contained less organic matter than the fat tubes in Mixed-T and unmixed arrays, e.g. in latter case 5.92% (thin tubes) against 8.13% (fat tubes; $p = 0.0022$; Table 2). The opposite trend was observed for Mixed-F: 7.32% in thin tubes and 5.97% in fat tubes ($p = 0.0293$; Table 2). On day 2, there was a significant difference in organic matter content for unmixed arrays only: 4.44% in thin tubes against 7.97% in fat tubes ($p = 0.0000$; Table 2).

Secondly, the median grain diameter was smaller on day 1 than on day 2 (Table 4). Whereas there was a substantial variability in grain size between arrays and also tube aspect ratios on day 1, the grain size trapped was closer to uniform on day 2. Indeed, on day 1, the thin tubes trapped finer particles than the fat tubes in unmixed arrays ($p = 0.0007$; Table 2). As a comparison, the median grain diameter of the surrounding surficial sediment was of 189.50 μm on day 1 and 193.00 μm on day 2.

Consistent with grain size results, the silt-clay content of the trapped sediment was much larger on day 1 than on day 2: between 15.10% and 24.08% on day 1 and between 5.54% and 9.43% on day 2 (Table 4). On day 1, only the unmixed arrays exhibit a clear difference: 15.10% for thin tubes against 24.08% for fat tubes ($p = 0.0016$; Table 2). On day 2, no clear trend was observed. As a comparison, the silt-clay content of the surrounding surficial sediment was of 11.47% on day 1, which is lower than the sediment captured in the tubes. On day 2, the trapped sediment exhibited a fines content similar to the surrounding surficial sediment (7.78%).

The number of tubes appeared to be negatively correlated with percentages of fines and TOM (total organic matter; Fig. 5). Linear regressions suggest a decrease in fines and TOM when the number of tubes increases, with coefficients of determination up to 0.88 for TOM on day 2 regardless of the aspect ratio (Fig. 5).

Background sediment deposition

To estimate the sediment deposition in each array, two tiles were inserted in the sediment bed at random positions. The amount of sediment deposited on the tiles in the control array was twice as much on day 1 than on day 2 (Fig. 6). The presence of tubes appeared to reduce the sediment deposition under the slightly rougher conditions of day 1. Indeed, on day 1, the sediment deposition was roughly twice as large in the control array than in the arrays that contain tubes (Fig. 6):

Table 3 Results of two-way analysis of variance (ANOVA) testing between aspect ratios differences in macro-organics and sediment deposition rates, organic matter and silt-clay contents of trapped sediment as well as median diameter d_{50} as a function of array. ANOVA provides probability values noted p that indicate if the variations between the tube contents are likely to stem from the sources of variability studied, i.e. aspect ratio and array, but also from their combined influence noted aspect ratio*array. Significant p values are in italics ($p < 0.05$, 95% confidence level). The table below also includes for each source the degrees of freedom (df), the mean squares (MS), that characterize how much the variations in tube content can be explained by the considered source, and the ratio of mean squares (F-statistic). The value called "error" shows the remaining variations in tube content that cannot be explained by the model

Day 1	Source	df	MS	F	p
Macro-organics deposition rates	Aspect ratio	1	280.4	17.69	*0.0000*
	Array	2	394.1	24.86	*0.0000*
	Aspect ratio *array	2	54.0	3.41	*0.0354*
	Error	172	15.9		
Sediment deposition rates	Aspect ratio	1	2932.3	3.75	0.0545
	Array	2	5434.0	6.95	*0.0013*
	Aspect ratio *array	2	4388.8	5.61	*0.0044*
	Error	170	782.1		
Silt-clay content	Aspect ratio	1	13.1	1.2	0.2897
	Array	2	17.0	1.57	0.2412
	Aspect ratio *array	2	72.6572	6.7	*0.0083*
	Error	15	10.8		
Organic matter content	Aspect ratio	1	7.3	10.09	*0.0059*
	Array	2	2.1	2.87	0.086
	Aspect ratio *array	2	7.3	10.04	*0.0015*
	Error	16	0.7		
d_{50}	Aspect ratio	1	93,388.9	0.08	0.7839
	Array	2	10,211,786.7	8.53	*0.0034*
	Aspect ratio *array	2	14,681,786.7	12.26	*0.0007*
	Error	15	1,197,811.1		
Day 2	Source	df	MS	F	p
Macro-organics deposition rates	Aspect ratio	1	1.8	15.56	*0.0001*
	Array	2	0.1	0.77	0.4665
	Aspect ratio *array	2	0.6	5.11	*0.0071*
	Error	149	0.1		
Sediment deposition rates	Aspect ratio	1	243.9	3.13	0.0790
	Array	2	73.1	0.94	0.3941
	Aspect ratio *array	2	436.6	5.59	*0.0045*
	Error	162	78.0		
Silt-clay content	Aspect ratio	1	2.7	2.74	0.1221
	Array	2	17.1	17.12	*0.0002*
	Aspect ratio *array	2	0.5	0.48	0.6276
	Error	13	1.0		
Organic matter content	Aspect ratio	1	7.1	12.68	*0.0026*
	Array	2	3.7	6.52	*0.0085*
	Aspect ratio *array	2	8.0	14.25	*0.0003*
	Error	16	0.6		
d_{50}	Aspect ratio	1	65,261.2	0.16	0.7001
	Array	2	275,334.4	0.65	0.5362
	Aspect ratio *array	2	492,480.0	1.17	0.341
	Error	13	420,935.9		

12.8 mg·cm^{-2} compared to 6.8 mg·cm^{-2}. On day 2, the sediment deposition in the control array and in the arrays with tubes except Mixed-F were alike, i.e. 7.5 mg·cm^{-2} and 5.7 mg·cm^{-2}, respectively (Fig. 6).
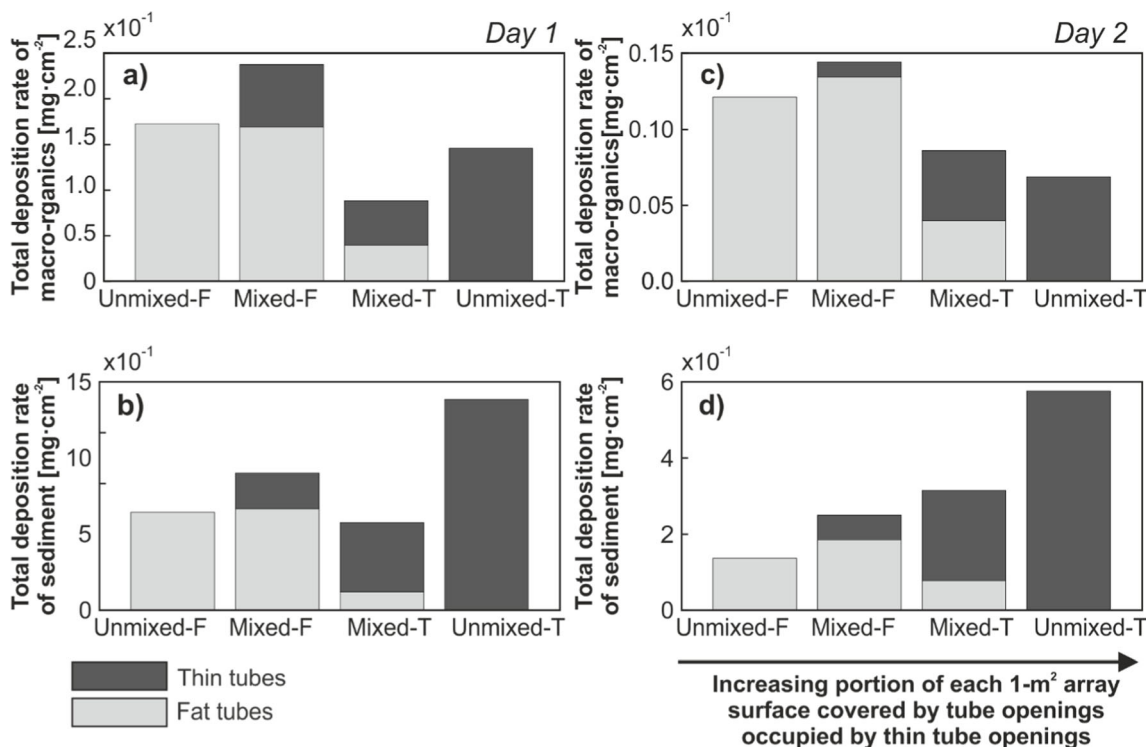
Fig. 4 Total deposition rates of macro-organic material and sediment captured per array. Graphs (**a**) and (**c**) show the deposition rate of macro-organics caught per array on day 1 and day 2, respectively. Graphs (**b**) and (**d**) show the sediment deposition rate per array on day 1 and day 2, respectively. The different arrays are sorted along the horizontal axis according to the area occupied by thin tube openings. Note the change in scale between left- and right-hand columns

Numerical simulations

Results of the 2D simulations of the hydrodynamics in the mimicked crab burrows are shown in Fig. 7. When the flow encounters the tube openings, turbulent kinetic energy is enhanced inside the tubes and along the sediment bed on the downstream side of the burrow (Fig. 7). For both aspect ratios,

stacked vortices develop inside the tubes: three distinct vortex cells form in the fat tubes, whereas four vortices form in the thin tubes (Fig. 7a, b). The penetration depth of the flow in "crab burrows" depends on the aspect ratio, with vortices reaching further down in fat tubes. However, only the uppermost vortex cell displays substantially enhanced TKE values. Moreover, this main vortex is more turbulent in fat than thin

Table 4 Mean (standard deviation) properties of trapped sediment. The content of several tubes was gathered randomly to have several replicates with sufficient amounts of material for the analysis of the trapped sediment properties. TOM stands for total organic matter

| Day	Array	Tube	Number of replicates	TOM (%)	Median grain size (μm)	Silt-clay (%)
Day 1	Unmixed	Thin	5	5.92 (0.85)	172.20 (6.30)	15.10 (2.81)
		Fat	6	8.13 (0.84)	141.00 (12.17)	24.08 (3.83)
	Mixed-F	Thin	2	7.32 (0.03)	163.50 (4.95)	18.92 (0.45)
		Fat	4	5.97 (0.69)	188.25 (15.76)	16.03 (3.78)
	Mixed-T	Thin	3	6.43 (0.14)	145.33 (8.02)	21.76 (2.72)
		Fat	2 for TOM − 1 otherwise	9.35 (1.93)	147.00 (−)	21.34 (−)
Day 2	Unmixed	Thin	5 for TOM − 3 otherwise	4.44 (0.70)	186.00 (6.08)	9.17 (1.73)
		Fat	6 for TOM − 5 otherwise	7.97 (0.70)	180.20 (8.76)	9.43 (1.00)
	Mixed-F	Thin	2	6.04 (0.27)	184.50 (6.36)	7.78 (0.76)
		Fat	4	5.75 (0.99)	189.75 (5.32)	9.15 (0.76)
	Mixed-T	Thin	3	4.49 (0.89)	186.33 (4.93)	5.54 (0.31)
		Fat	2	4.97 (0.04)	184.50 (0.71)	6.31 (0.69)
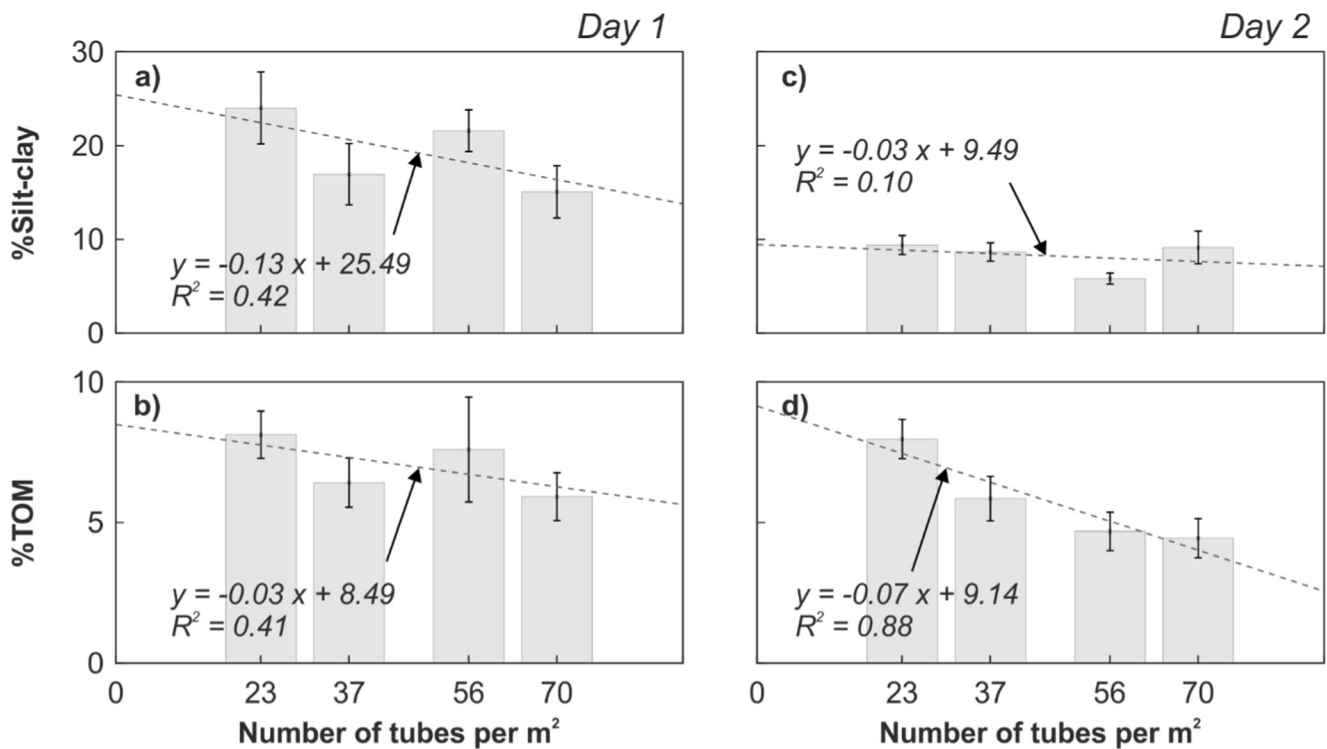
Fig. 5 Change in sediment properties with number of tubes. **a** and **c** correspond to the relationship between the silt-clay content (%) of the sediment trapped in the tubes (fat and thin tubes taken together) and the number of tubes per m^2 on day 1 and day 2, respectively. **b** and **d** correspond to the relationship between the organic matter content (%) of the sediment trapped in the tubes (fat and thin tubes taken together) and the number of tubes per m^2 on day 1 and day 2, respectively. In all graphs, the dashed line shows the results of the linear regression

tubes. Outside of the tubes, the turbulence generated by the interaction of the flow with the tube openings appears more intense but of shorter duration (more quickly dissipated) for the fat than thin tubes, as indicated by the higher TKE values downstream (Fig. 7).

Vertical velocity profiles are logarithmic above the bed mimicking the applied inflow conditions (Fig. 7c). Mean horizontal velocities ($\bar{U}_X$) within the tubes exhibit perturbations to this profile occurring down to $Z = 3.3$ cm and $Z = 1.9$ cm for fat and thin tubes, respectively (Fig. 7c, d). In addition, mean horizontal velocity profiles ($\bar{U}_Z$) are asymmetrical around the tube centreline at 1 cm below the tube openings in both tubes (Fig. 7d). Downward velocities of up to 7.8 mm·s^{-1} could be

observed at the downstream side of the fat tube whereas upward velocities of 4.9 mm·s^{-1} occur at the upstream side. Similarly, downward velocities at the downstream side of the thin tube reach values of 2.1 mm·s^{-1} and upward velocities are up to 1.6 mm·s^{-1} at the upstream side of the thin tube.

Discussion

The present study demonstrates that crab burrows can capture macrofauna (e.g. crabs), organic material and sediments. Macro-organics and sediment were found in the tubes for both days. However, our results revealed that the total amount of
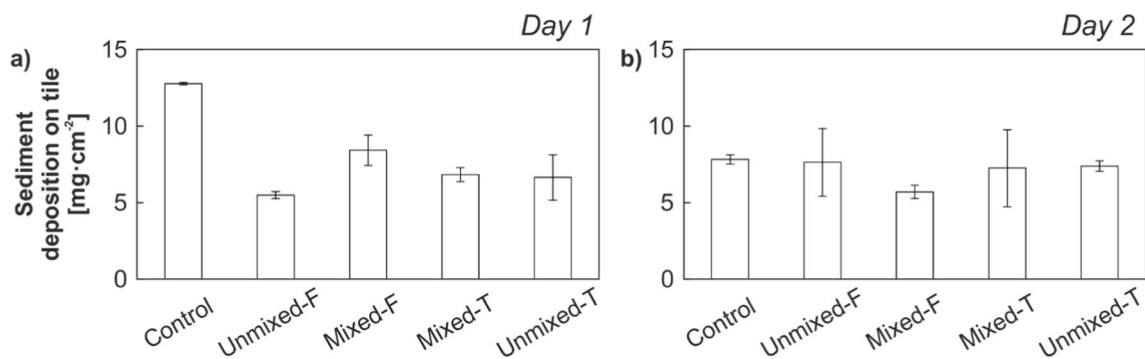

Fig. 6 Sediment deposition in mg·cm^{-2} estimated for each array from the tiles. The different arrays are sorted along the horizontal axis with increasing numbers of thin tubes to the right. Vertical lines plotted at the top of the bars correspond to the standard errors
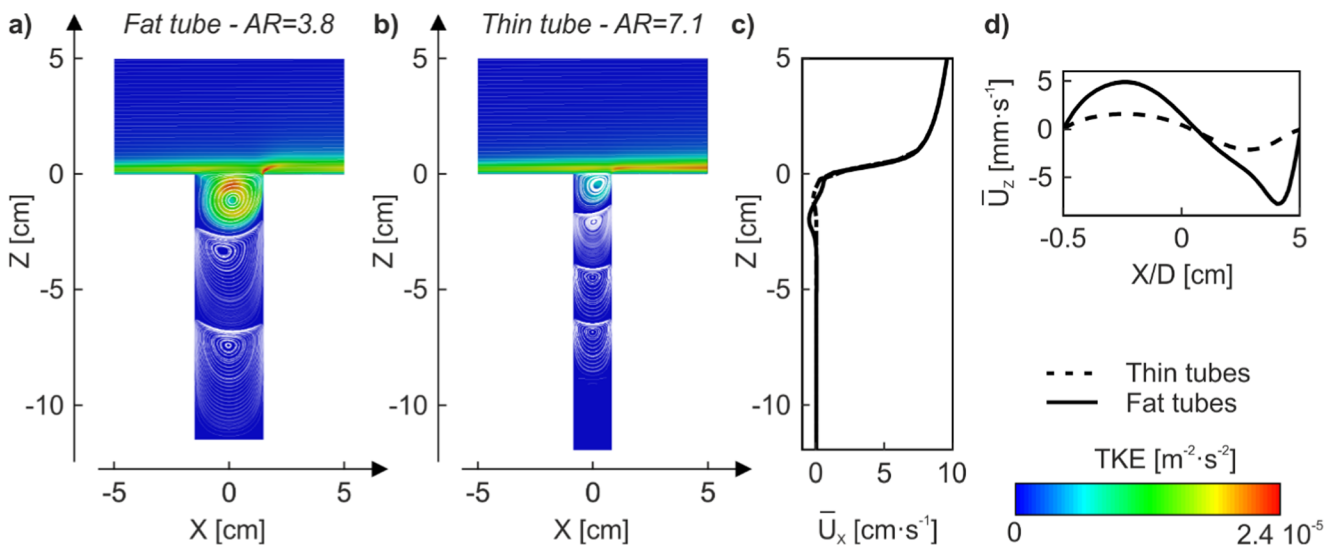
Fig. 7 Results of the 2D simulations with OpenFOAM. **a** Screenshot of the flow pattern in the fat tube (aspect ratio of 3.8) plotted with Paraview. **b** Screenshot of the flow pattern in the thin tube (aspect ratio of 7.1) plotted with Paraview. **c** Downstream velocity profiles (along X-axis) extracted along Z-axis at the centre of the tubes, i.e. X = 0 cm. **d** Vertical velocity profiles (along Z-axis) extracted along X-axis at the centre of the tube openings and Z = − 1 cm. **d** corresponds to the tube diameter and AR stands for aspect ratio

material caught in burrows is strongly dependent on the hydrodynamic conditions, as currents control the quantity of material in suspension in the water column (Fig. 3). Stronger hydrodynamic conditions led to greater TSS in water column (Fig. 2) and, hence, more material was available for capture. In particular, the sharp increase in TSS at the ebb tide on day 1 is likely to contribute to the difference in material capture between the 2 days of experiments.

Additionally, the amount of material collected and the associated deposition rates are also related to the aspect ratio of crab burrows (Fig. 8a). Burrow arrays appear to play a major role on capture capacity of organic material and sediment. The array configuration also seems to control the trapped sediment organic matter content as well as the capture of different sediment type fractionations (Fig. 8b).

Influence of aspect ratio on capture efficiency

Macrofrauna was caught in all arrays by both types of tubes: fat tubes with an aspect ratio of 3.8 and thin tubes with an aspect ratio of 7.1. Based on the number of arrays, and short term of deployment, a detailed analysis is neglected; thus, we would need rather long-term monitoring to assess the link between macrofauna and burrow aspect ratio. However, in general, more crabs were caught in the fat tubes than in the thin tubes.

Our results suggest that the aspect ratio is a key factor controlling the catching of large organic material. Indeed, fat tubes caught larger amounts (dry weight) of macro-organics than thin tubes on both days and across all arrays (Fig. 3; Table 2). Arrays containing the greatest numbers of fat tubes (Unmixed-F with 23 fat tubes and Mixed-F with 16 fat tubes)

were the most efficient at trapping organics. Moreover, on day 1, fat tubes tended to catch much bigger pieces of macro-organic material than thin tubes, which can be explained by the wider openings of fat tubes allowing capture of larger pieces of material. Hence, the capture of macro-organics is a selective process. To extrapolate the results of catching of macro-organics to a larger tidal flat area, we assume that our two mixed scenarios mimic more realistic natural burrow morphology and density conditions (Needham et al. 2010, 2013). A simple upscaling gives an amount of macro-organics captured by crab burrows for a fat tube-dominated tidal flat (Mixed-F) of approximately 2.4 t·km^{-2} and for a thin tube-dominated field (Mixed-T) of approximately 0.9 t·km^{-2} macro-organics over a tidal cycle.

This study highlights that tubes clearly enhance sediment capture compared to the surrounding bed. Indeed, the sediment deposition rates appear to be greater in both types of crab burrows (fat tubes and thin tubes) than on the tiles placed on the bed in-between (Fig. 4 and Fig. 7). This result supports previous observations that burrows dug by crabs increase the sediment capture (Botto et al. 2006; Escapa et al. 2008; Iribarne et al. 1997, 2000). Associated with this larger amount of sediment trapping is an increase of trapped organic matter (Table 4), and thus more food provided to the benthic

Fig. 8 Main findings. **a** Material capture in single burrows. Greater ▶ amounts of macro-organics, as well as sediment, are collected in fat tubes. Fat tubes catch larger organic elements since they have a wider opening. The hydrodynamic conditions determine the quantity of material available for trapping in the water column. **b** Turbulence generation and sediment trapping in arrays of burrows. A larger number of tubes appears to generate more intense turbulence, which keeps fine material, i.e. organic matter and fine sediment particles, in suspension
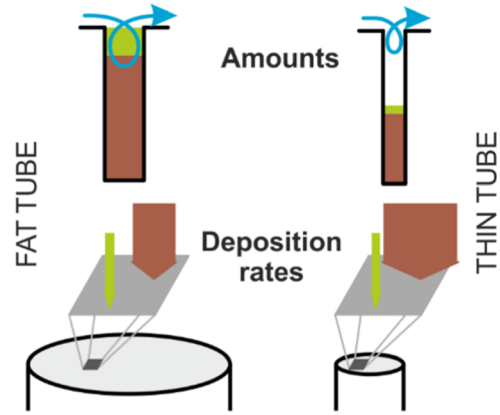
a) SINGLE BURROW

CALM CONDITIONS

*Low sediment concentration* **+** *Small macro-organics in motion*

FAT TUBE

Amounts

THIN TUBE

Deposition rates
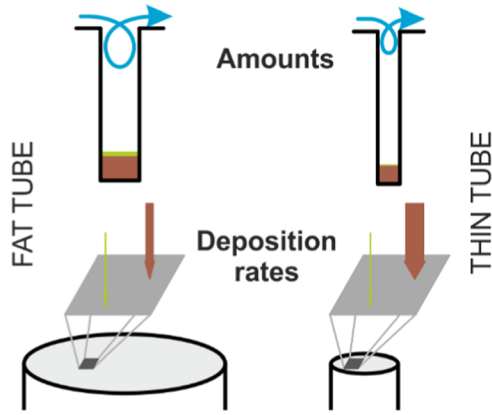
ROUGH CONDITIONS

High sediment concentration **+** *Big and small macro-organics in motion*

FAT TUBE

Amounts

THIN TUBE

Deposition rates

Legend: ↻→ Flow pattern ▮ Macro-organics ▮ Sediment

b) ARRAY OF BURROWS

Turbulences rise with increasing number of burrows i.e. obstructions

Unmixed-F

Mixed-F

Unmixed-T
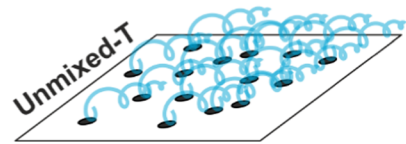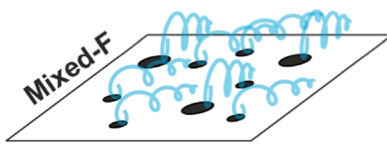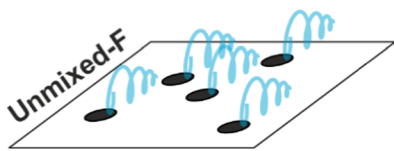
Reduced turbulences enhance settling of fine material i.e. organic matter and silt-clay ⟷ Greater turbulences prevent fines i.e. organic and silt-clay particles from settling

"far-field" impact
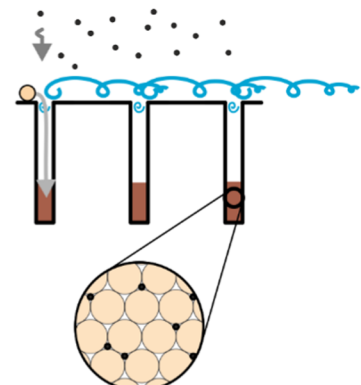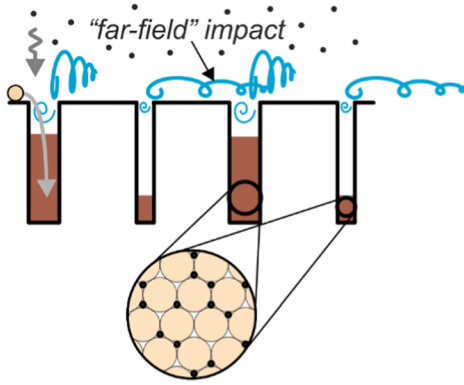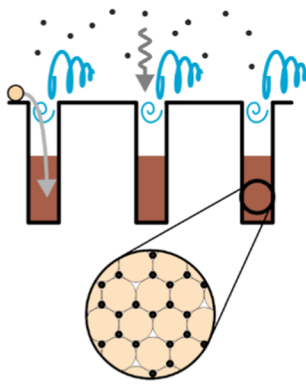
Turbulence level dependent on burrow array configuration **+** Trapping of fine material controlled by turbulence ➡ **Key role of burrow array configuration in sediment fractionation**

Legend: ↻ Vortex 〰 Turbulence ▮ Sediment ◯ Sand • Silt-clay

communities living in the burrows (Botto and Iribarne 2000; Botto et al. 2006). However, further investigations are required to gain a deeper insight into the food chain of tunnelling mud crabs similar to studies by Botto et al. (2006).

Comparison of dry weight of sediment trapped in crab burrows with different aspect ratios showed that the fat tubes captured the highest amounts in all arrays and for both days, similar to macro-organics (Fig. 3; Table 2). This observation supports the findings of Gardner (1980a), who demonstrated a positive correlation between the deposition rate of particles collected in cylindrical traps and the aspect ratio. In addition, these values are in the same order of magnitude reported in former studies for *Neohelice granulata* crab burrows (Escapa et al. 2008). Here, dry weight sediment deposition rate of around 108 mg·cm^{-2} was measured in a tubular-shaped burrows with an aspect ratio of 4 during one tidal cycle on a sandflat.

In addition to the clear differentiations of amount of sediments and sediment deposition rate between fat and thin crab burrow, the discrepancy in sediment composition was the strongest between fat and thin tubes in unmixed arrays. In mixed arrays, organic matter content, median diameter d$_{50}$ and silt-clay percentage of trapped sediments did not significantly differ between the two tested aspect ratios.

Furthermore, our numerical simulations demonstrate that thin tubes influence flow patterns further downstream than fat tubes. So, thin burrows may have a greater "far-field" impact and hence, have a stronger influence on the surrounding burrows compared to single fat tubes. The penetration depth of vortices correlates to first order with the diameter of the burrow, which is in good agreement with previous studies (Weiss and Florsheim 1965; O'Brien 1972). These simulations reveal that a faster downward flow may promote greater amounts of material entering fat tubes than thin tubes. This result supports previous findings stating that the aspect ratio of cylindrical traps is the key factor for collection of sediment particles (Gardner 1980a). In addition to the higher TSS on day 1, the fact that "the trapping efficiency of cylinders may increase slightly with increasing current velocity" (Gardner 1980a) may contribute to the larger capture rates observed on day 1 (Fig. 3). However, further simulations would be required to distinguish between the individual influences of flow speeds and suspended sediment concentrations. In addition, pellets, tracks and even animal bodies can change the roughness of the bed, i.e. micro-topography, leading to an increase in turbulence that is likely to push water into burrows and to enhance their flushing rate (Ziebis et al. 1996). Furthermore, a grain of fine sand (d$_{50}$ = 180 μm), typical of the sampled surficial sediment, settles at a velocity of 21 mm·s^{-1} (Grace 1986); and hence, such sediment particles are too heavy to be re-inserted in the water column by the upward outflow. Consequently, fine sand would be trapped in both tubes. In contrast a finer medium silt sediment (d$_{50}$ =

25 μm), which constituted the majority of trapped sediment on day 1, would not be trapped neither in fat nor thin tubes in our simulations as such grains have a settling velocity of 0.8 mm·s^{-1}. Flow speeds inside the tubes appear to be strong enough to carry such a sediment particle out of the crab burrow for both aspect ratios. However, some fine particles may be trapped when they collide with burrow walls or when they get advected deeper into the tube and eventually reach a place where they can settle out. Generally, numerical simulations suggest that the aspect ratio is not a dominant factor for trapping fine sediments.

Influence of burrow arrays — field observations

In all test arrays, the area occupied by tube openings was constant (Fig. 1a). However, our results showed that the array configuration affects the total deposition rates of sediment and macro-organics. The latter is mainly controlled by the absolute number of fat tubes per area. We focus in the following on sediment trapping behaviour as a function of array composition. Indeed, the impact of the array configuration and, hence, crab burrow distribution on sediment capture appears to be a function of number, as well as distribution of, fat versus thin tubes (Fig. 8b).

Our findings showed that the number of thin tubes control the total sediment deposition rates and hence the sediment capture particularly on day 2 (Fig. 4). Thus, the sediment deposition rate is always greater in Unmixed-T array with thin tubes compared to Unmixed-F with fat tubes (Fig. 3 and Fig. 5). In addition, homogeneous thin tubes array (Unmixed-T) always exhibit the largest sediment deposition rate independent of weather conditions. Moreover, sediment deposition rate always increased when adding a few thin tubes to the homogeneous fat array (e.g. the Mixed-F scenario) during both days. More thin tubes result in an increase of absolute sediment deposition rate only during calm conditions (day 2).

A simple upscaling of our experimental results provides an estimate of the amount of sediment captured by crab burrows (with a distribution of aspect ratios similar to Unmixed-T) as roughly 14 t·km^{-2} over one tidal cycle. For this calculation, a similar sediment supply is assumed for all burrows whereas, in natural conditions, as sediment is deposited, there is less sediment available for deposition downstream. Such estimated sediment volumes may have significant impacts, on the geomorphology of intertidal sandflats, by for example, altering erosion properties. In addition to the impact of aspect ratio distribution on sediment capture and deposition rate, a decrease of fine content and organic matter content could be identified, associated with an increasing number of crab burrows per array (Table 4). This result suggests that the turbulence level or TKE not only controls the capture capacity, rather it also causes a sediment fractionation. Indeed, reduced trapping of fines may stem from enhanced turbulence that

keeps the sediment in suspension. This observation was more pronounced during rough weather conditions on day 1 compared to the calmer day 2. Such a muddification process has already been described for seagrass beds (van Katwijk et al. 2010). Therefore, even in sandy environments, the sediments trapped in crab burrows were finer than the surrounding substrate. Crab burrows in sandy sediments have a shorter permanency than in muddy substrates (Needham et al. 2011). Thus, when crab burrows collapse, the surficial sediment may become muddier over time, and hence alter the erosion properties. However, neither muddification nor significant changes in erosional behaviour were observed in our target area. Hence, trapped sediment may be reintroduced in the system due to waves that rework the sediment bed and re-suspend the fine grains, but also owing to the crabs excavating the trapped sediment during the maintenance of their burrows.

Based on our numerical simulations, we identified the aspect ratio and particularly the "far-field" impact of thin tubes as a potential controlling factor for sediment trapping. The fat tubes in Unmixed-F are more likely to affect individually the flow and behave as an isolated roughness element; as the fewer tubes (23 tubes) were sparsely scattered. Conversely, thin tubes influence the flow pattern in the vicinity including the surrounding tubes owing to their "far-field" impact, thus causing interactions between the wakes and eddies generated by burrows. Therefore, for arrays with many tubes (e.g. Unmixed-T arrays with 70 tubes), we expect enhancement in TKE owing to burrow density. Such an increase in turbulence generation by biogenic structures and associated effects on sedimentation was observed in the field for a wide range of biogenic structures (Green 2005; Nepf 2012), such as mangrove roots density (Mullarney et al. 2017; Norris et al. 2017,

2019) or of artificial epibenthic structures (Bouma et al. 2007). The interactions between a flow and emergent structures at different densities modify the shear stress, leading to differences in sedimentation. A skimming flow may develop when the burrow density is high enough (Nowell and Church 1979; Eckman 1983; Nowell and Jumars 1984; Friedrichs et al. 2000, 2009; Coco et al. 2006). However, additional experiments are required to further unravel the link between burrow density and flow regime for different burrow aspect ratios as the significance of the sediment deposition rates are not yet sufficiently convincing for different array configurations. Homogenous arrays of burrows (only one aspect ratio) at different densities could be studied following the strategy of Eckman et al. (1981) to determine the impact of animal tubes on sediment stabilization.

Conclusions and outlook

In this paper, we showed that tubes mimicking *Austrohelice crassa* crab burrows (similar dimensions and shape) act as passive traps of macrofauna, macro-organics and sediment. Therefore, such benthic structures and their builders are expected to impact their ecosystem by enhancing food deposition that would benefit the benthic communities living in these cavities. In addition, these ecosystem engineers are also likely to change the properties of the sediment they live in over short time scales (days) since more fine particles were captured. Through maintenance activities, *Austrohelice crassa* crabs remove the particles trapped in their burrows instead of keeping them inside. Since burrow excavation (clearing) only occurred at low tide, i.e. when burrows are exposed to air, the results
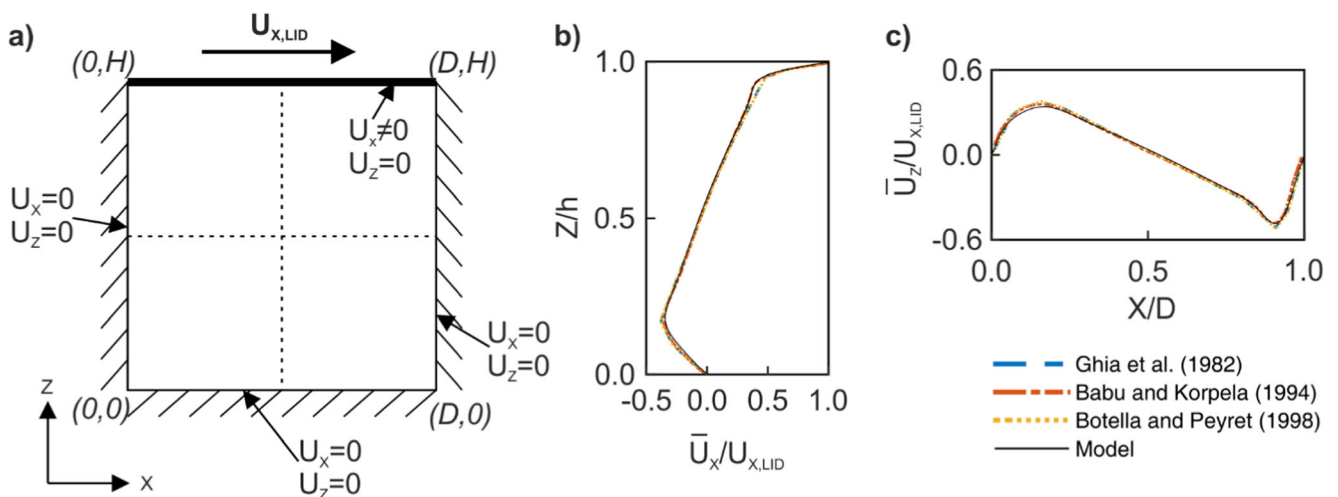
Fig. 9 Geometry and flow validation of hydrodynamics in square cavity at Re = 1000. **a** Boundary conditions and geometry of the square cavity (height H equal to diameter D). **b** Modelled results of mean streamwise velocity plotted against published data. Data were extracted along a vertical profile located at X/D = 0.5. **c** Modelled results of mean vertical velocity plotted against published data. Data were extracted along a horizontal profile located at Z/H = 0.5

presented in this study are not only specific for empty burrows.

In particular, this paper demonstrated that the burrow aspect ratio is a controlling factor for the capture of macrofauna, macro-organics as well as sediment at both the scale of a single tube and at the scale of an array of tubes. Indeed, burrows with small aspect ratio (fat tubes) trap larger amounts of macrofauna, macro-organics and sediments than burrows with a high aspect ratio (thin tubes). In addition, tubes with wider opening catch larger pieces of macro-organics. When normalised by opening area, burrows with a small aspect ratio (fat tubes) exhibit a larger deposition rate of macro-organics.

A greater number of thin tubes per array is associated with more sediment trapping and, thus, burrows with high aspect ratio (thin tubes) seem to dominate the sediment capture in burrow arrays. In case of homogeneous array configurations, burrows with a small aspect ratio (fat tubes) have a smaller trapping rate compared to burrows with a high aspect ratio (thin tubes). In contrast, for mixed arrays, no clear difference of sediment deposition rate was observed between fat and thin burrows.

In addition, the thin burrows have a greater "far-field" impact, in which flow disturbances from multiple burrows interact, thus enhancing turbulence. Therefore, an increase in turbulence is associated with the number of thin tubes per array. This turbulence enhancement generates hydrodynamic conditions that prevent fine particles from settling. Conversely, the turbulence decreases with a smaller number of thin tubes, which facilitates deposition of fines within burrows and, thus, larger amounts of fine sediment fractions are captured.

However, the selective capture in burrow arrays with different configurations needs further investigation. New techniques are required for in situ measurements to overcome technical limitations encountered during field measurements. Indeed, it is difficult to measure small-scale flow features (vortices) and quantify fluid exchange rate into and out of the burrows in a field setting. Furthermore, to assess the significance of material capture within arrays, more replicates of array configuration should be deployed. The differences in turbulent dissipation rate above the tested arrays were small and, therefore, it is impossible to attribute these changes to array properties rather than to metre-scale spatial variability of flow conditions. Numerical simulations would help to assess the significance of these results by utilising the same setup as the one employed in the field.

Model setup and validation

In order to verify and validate the numerical model, several benchmark tests were conducted. According to Oberkampf and Trucano (2008), the simulation of a same case should be run for three different grid sizes as well as three different time steps. In addition, numerical data should be compared with experimental data (numerical, flume or field) to ensure that the model output corresponds to the reality and that its accuracy is in an acceptable or reasonable range. A large number of studies have already been published regarding the flow in cavities: 2D or 3D lid-driven cavity flow in square/cubic or rectangular cavities (Ghia et al. 1982; Ku et al. 1987), flow past open cavities with different shapes (Ozalp et al. 2010). In order to validate our simple model, a square unit cavity and a rectangular cavity were generated. The geometry, as well as the boundary conditions, is shown (Fig. 9a). In total, a set of nineteen numerical experiments was conducted. Nine Reynolds numbers were considered, ranging from 100 to 100,000. A vertical profile of mean streamwise velocity was extracted at $X/D = 0.5$ and an horizontal profile of mean vertical velocity was extracted at $Z/H = 0.5$, where X and Z refer to the horizontal and vertical axes, respectively, and, D and H are the length and the height of the cavity, respectively. These profiles were plotted against data from Ghia et al. (1982), Takemoto et al. (1984), Babu and Korpela (1994), Cortes and Miller (1994) and Botella and Peyret (1998). The results of our model validation exhibited good agreement with these numerical data for mean flow speeds and vortex structure (Fig. 9b, c).

References

Babu V, Korpela SA (1994) Numerical solution of the incompressible three-dimensional Navier-Stokes equations. Comput Fluids 23: 675–691. https://doi.org/10.1016/0045-7930(94)90009-4

Botella O, Peyret R (1998) Benchmark spectral results on the lid-driven cavity flow. Comput Fluids 27:421–433. https://doi.org/10.1016/S0045-7930(98)00002-4

Botto F, Iribarne O (2000) Contrasting effects of two burrowing crabs (*Chasmagnathus granulata* and *Uca uruguayensis*) on sediment composition and transport in estuarine environments. Estuar Coast Shelf Sci 51:141–151. https://doi.org/10.1006/ecss.2000.0642

Botto F, Iribarne O, Gutierrez J, Bava J, Gagliardini A, Valiela I (2006) Ecological importance of passive deposition of organic matter into burrows of the SW Atlantic crab *Chasmagnathus granulatus*. Mar Ecol Prog Ser 312:201–210. https://doi.org/10.3354/meps312201

Bouma T, Van Duren L, Temmerman S, Claverie T, Blanco-Garcia A, Ysebaert T, Herman P (2007) Spatial flow and sedimentation patterns within patches of epibenthic structures: Combining field, flume and modelling experiments. Cont Shelf Res 27:1020–1045. https://doi.org/10.1016/j.csr.2005.12.019

Butman CA (1986) Sediment trap biases in turbulent flows: results from a laboratory flume study. J Mar Res 44:645–693. https://doi.org/10.1357/002224086788403051

Butman CA, Grant WD, Stolzenbach KD (1986) Predictions of sediment trap biases in turbulent flows: a theoretical analysis based on observations from the literature. J Mar Res 44:601–644. https://doi.org/10.1357/002224086788403024

Coco G, Thrush SF, Green MO, Hewitt JE (2006) Feedbacks between bivalve density, flow, and suspended sediment concentration on patch stable states. Ecology 87:2862–2870. https://doi.org/10.1890/0012-9658(2006)87[2862:FBBDFA]2.0.CO;2

Cortes A, Miller J (1994) Numerical experiments with the lid driven cavity flow problem. Comput Fluids 23:1005–1027. https://doi.org/10.1016/0045-7930(94)90002-7

Eckman JE (1983) Hydrodynamic processes affecting benthic recruitment. Limnol Oceanogr 28:241–257. https://doi.org/10.4319/lo.1983.28.2.0241

Eckman JE, Nowell AR, Jumars PA (1981) Sediment destabilization by animal tubes. J Mar Res 39:361–373

Escapa M, Perillo GM, Iribarne O (2008) Sediment dynamics modulated by burrowing crab activities in contrasting SW Atlantic intertidal habitats. Estuar Coast Shelf Sci 80:365–373. https://doi.org/10.1016/j.ecss.2008.08.020

Friedrichs M, Graf G, Springer B (2000) Skimming flow induced over a simulated polychaete tube lawn at low population densities. Mar Ecol Prog Ser 192:219–228. https://doi.org/10.3354/meps192219

Friedrichs M, Leipe T, Peine F, Graf G (2009) Impact of macrozoobenthic structures on near-bed sediment deposition rates. J Mar Syst 75:336–347. https://doi.org/10.1016/j.jmarsys.2006.12.006

Gardner WD (1980a) Field assessment of sediment traps. J Mar Res 38:41–52

Gardner WD (1980b) Sediment trap dynamics and calibration: a laboratory evaluation. J Mar Res 38:17–39

Gardner WD (1985) The effect of tilt on sediment trap efficiency. Deep Sea Research Part A. Oceanogr Res Pap 32:349–361. https://doi.org/10.1016/0198-0149(85)90083-4

Ghia U, Ghia KN, Shin C (1982) High-Re solutions for incompressible flow using the Navier-Stokes equations and a multigrid method. J Comput Phys 48:387–411. https://doi.org/10.1016/0021-9991(82)90058-4

Gibbs M, Thrush S, Ellis J (2001) Terrigenous clay deposition on estuarine sandflats: using stable isotopes to determine the role of the mud crab, Helice crassa Dana, in the recovery process. Isot Environ Health Stud 37:113–131. https://doi.org/10.1080/10256010108033288

Gilbert F, Aller RC, Hulth S (2003) The influence of macrofaunal burrow spacing and diffusive scaling on sedimentary nitrification and denitrification: an experimental simulation and model approach. J Mar Res 61:101–125. https://doi.org/10.1357/002224003321586426

Grace JR (1986) Contacting modes and behaviour classification of gas-solid and other two-phase suspensions. Can J Chem Eng 64:353-363.https://doi.org/10.1002/cjce.5450640301

Graf G, Rosenberg R (1997) Bioresuspension and biodeposition: a review. J Mar Syst 11:269–278. https://doi.org/10.1016/S0924-7963(96)00126-1

Green JC (2005) Comparison of blockage factors in modelling the resistance of channels containing submerged macrophytes. River Res Appl 21:671-686. https://doi.org/10.1002/rra.854

Heron S, Ridd P (2001) The use of computational fluid dynamics in predicting the tidal flushing of animal burrows. Estuar Coast Shelf Sci 52:411–421. https://doi.org/10.1006/ecss.2000.0761

Heron S, Ridd P (2003) The effect of water density variations on the tidal flushing of animal burrows. Estuar Coast Shelf Sci 58:137–145. https://doi.org/10.1016/S0272-7714(03)00068-4

Heron S, Ridd P (2008) The tidal flushing of multiple-loop animal burrows. Estuar Coast Shelf Sci 78:135–144. https://doi.org/10.1016/j.ecss.2007.11.018

Iribarne O, Bortolus A, Botto F (1997) Between-habitat differences in burrow characteristics and trophic modes in the southwestern Atlantic burrowing crab Chasmagnathus granulata. Mar Ecol Prog Ser 155:137–145. https://doi.org/10.3354/meps155137

Iribarne O, Botto F, Martinetto P, Gutierrez JL (2000) The role of burrows of the SW Atlantic intertidal crab Chasmagnathus granulata in trapping debris. Mar Pollut Bull 40:1057–1062. https://doi.org/10.1016/S0025-326X(00)00058-8

Kristensen E & Kostka J (2005) Macrofaunal burrows and irrigation in marine sediment: microbiological and biogeochemical interactions. Interactions between Macro-and Microorganisms in Marine Sediments, pp 125–157. https://doi.org/10.1029/CE060p0125

Ku HC, Hirsh RS, Taylor TD (1987) A pseudospectral method for solution of the three-dimensional incompressible Navier-Stokes equations. J Comput Phys 70:439–462. https://doi.org/10.1016/0021-9991(87)90190-2

Laverock B, Gilbert JA, Tait K, Osborn AM, Widdicombe S (2011) Bioturbation: impact on the marine nitrogen cycle. Portland Press Limited. https://doi.org/10.1042/BST0390315

Le Hir P, Monbet Y, Orvain F (2007) Sediment erodability in sediment transport modelling: can we account for biota effects? Cont Shelf Res 27:1116–1142. https://doi.org/10.1016/j.csr.2005.11.016

Le Minor M, Bartzke G, Zimmer M, Gillis LG, Helfer V, Huhn K (2019) Numerical modelling of hydraulics and sediment dynamics around mangrove seedlings: Implications for mangrove establishment and reforestation. Estuar Coast Shelf Sci 217:81-95. https://doi.org/10.1016/j.ecss.2018.10.019

Meadows PS, Meadows A, Murray JM (2012) Biological modifiers of marine benthic seascapes: their role as ecosystem engineers. Geomorphology 157:31–48. https://doi.org/10.1016/j.geomorph.2011.07.007

Morrisey D, Dewitt T, Roper D, Williamson R (1999) Variation in the depth and morphology of burrows of the mud crab Helice crassa among different types of intertidal sediment in New Zealand. Mar Ecol Prog Ser 182:231–242. https://doi.org/10.3354/meps182231

Mullarney JC, Henderson SM, Norris BK, Bryan KR, Fricke AT, Sandwell DR, Culling DP (2017) A question of scale: how turbulence around aerial roots shapes the seabed morphology in mangrove forests of the Mekong Delta. Oceanography 30:34–47. https://doi.org/10.5670/oceanog.2017.312

Murray JM, Meadows A, Meadows PS (2002) Biogeomorphological implications of microscale interactions between sediment geotechnics and marine benthos: a review. Geomorphology 47:15–30. https://doi.org/10.1016/S0169-555X(02)00138-1

Needham H, Pilditch C, Lohrer A, Thrush S (2010) Habitat dependence in the functional traits of Austrohelice crassa, a key bioturbating species. Mar Ecol Prog Ser 414:179–193. https://doi.org/10.3354/meps08726

Needham HR, Pilditch CA, Lohrer AM, Thrush SF (2011) Context-specific bioturbation mediates changes to ecosystem functioning. Ecosystems 14:1096–1109. https://doi.org/10.1007/s10021-011-9468-0

Needham HR, Pilditch CA, Lohrer AM, Thrush SF (2013) Density and habitat dependent effects of crab burrows on sediment erodibility. J Sea Res 76:94–104. https://doi.org/10.1016/j.seares.2012.12.004

Nepf HM (2012) Flow and Transport in Regions with Aquatic Vegetation. Annu Rev Fluid Mech 44:123-142. https://doi.org/10.1146/annurev-fluid-120710-101048

Nickell L, Atkinson R, Hughes D, Ansell A, Smith C (1995) Burrow morphology of the echiuran worm Maxmuelleria lankesteri (Echiura: Bonelliidae), and a brief review of burrow structure and related ecology of the Echiura. J Nat Hist 29:871–885. https://doi.org/10.1080/00222939500770311

Norris BK, Mullarney JC, Bryan KR, Henderson SM (2017) The effect of pneumatophore density on turbulence: a field study in a *Sonneratia*-dominated mangrove forest, Vietnam. Cont Shelf Res 147:114–127. https://doi.org/10.1016/j.csr.2017.06.002

Norris BK, Mullarney JC, Bryan KR, Henderson SM (2019) Turbulence within natural mangrove pneumatophore canopies. J Geophys Res Oceans 124:2263–2288. https://doi.org/10.1029/2018JC014562

Nowell AR, Church M (1979) Turbulent flow in a depth-limited boundary layer. J Geophys Res Oceans 84:4816–4824. https://doi.org/10.1029/JC084iC08p04816

Nowell A, Jumars P (1984) Flow environments of aquatic benthos. Annu Rev Ecol Syst 15:303–328. https://doi.org/10.1146/annurev.es.15.110184.001511

Oberkampf WL, Trucano TG (2008) Verification and validation benchmarks. Nucl Eng Des 238:716–743. https://doi.org/10.1016/j.nucengdes.2007.02.032

O'Brien V (1972) Closed streamlines associated with channel flow over a cavity. Phys Fluids 15:2089–2097. https://doi.org/10.1063/1.1693840

Ozalp C, Pinarbasi A, Sahin B (2010) Experimental measurement of flow past cavities of different shapes. Exp Thermal Fluid Sci 34:505–515. https://doi.org/10.1016/j.expthermflusci.2009.11.003

Palau-Salvador G, Stoesser T, Fröhlich J, Kappler M, Rodi W (2010) Large eddy simulations and experiments of flow around finite-height cylinders. Flow Turbul Combust 84:239. https://doi.org/10.1007/s10494-009-9232-0

Spalding DB (1961) A Single Formula for the "Law of the Wall". J Appl Mech 28:455-458. https://doi.org/10.1115/1.3641728

Takemoto Y, Abe Y, Naitou H & Yamabe H (1984) On the third-order upwind finite-difference scheme in numerical analysis for initial-value problems. Nagoya Univ.(Japan). Inst. of Plasma Physics

Thrush SF, Hewitt JE, Norkko A, Cummings VJ, Funnell GA (2003) Macrobenthic recovery processes following catastrophic sedimentation on estuarine sandflats. Ecol Appl 13:1433–1455. https://doi.org/10.1890/02-5198

Van Katwijk M, Bos A, Hermus D, Suykerbuyk W (2010) Sediment modification by seagrass beds: muddification and sandification induced by plant cover and environmental conditions. Estuar Coast Shelf Sci 89:175–181. https://doi.org/10.1016/j.ecss.2010.06.008

Vopel K, Hancock N (2005) More than just a crab hole. Water Atmos 13:18–19

Warren JH, Underwood A (1986) Effects of burrowing crabs on the topography of mangrove swamps in New South Wales. J Exp Mar Biol Ecol 102:223–235. https://doi.org/10.1016/0022-0981(86)90178-4

Weiss RF, Florsheim BH (1965) Flow in a cavity at low Reynolds number. Phys Fluids 8:1631–1635. https://doi.org/10.1063/1.1761474

Widdows J, Brinsley M (2002) Impact of biotic and abiotic processes on sediment dynamics and the consequences to the structure and functioning of the intertidal zone. J Sea Res 48:143–156. https://doi.org/10.1016/S1385-1101(02)00148-X

Wiles PJ, Rippeth TP, Simpson JH, Hendricks PJ (2006) A novel technique for measuring the rate of turbulent dissipation in the marine environment. Geophys Res Lett 33. https://doi.org/10.1029/2006GL027050

Witbaard R, Duineveld G (1989) Some aspects of the biology and ecology of the burrowing shrimp *Callianassa subterranea* (Montagu) (*Thalassinidea*) from the southern North Sea. Sarsia 74:209–219. https://doi.org/10.1080/00364827.1989.10413430

Yager PL, Nowell AR, Jumars PA (1993) Enhanced deposition to pits: a local food source for benthos. J Mar Res 51:209–236. https://doi.org/10.1357/0022240933223819

Ziebis W, Forster S, Huettel M, Jorgensen B (1996) Complex burrows of the mud shrimp *Callianassa truncata* and their geochemical impact in the sea bed. Nature 382:619. https://doi.org/10.1038/382619a0